

# Optimizing tilt angles for enhanced solar PV output: A techno-environmental case study across Syrian cities

Ayman Abdul Karim Alhijazi<sup>1</sup>, Samer Diab<sup>2</sup>, Adil Adam<sup>3\*</sup>

<sup>1</sup> Faculty of Mechatronics Engineering, Al-Shamal Private University, Sarmadā 5P9P+6CP, Syria

<sup>2</sup> Engineering Department, Al-Zaytoonah International University, Azaaz 963-21, Syria

<sup>3</sup> Engineering Department, Al Zahraa University, Jarablus R2G5+38J, Syria

\* **Corresponding author:** Adil Adam, [adiladam080@gmail.com](mailto:adiladam080@gmail.com)

## CITATION

Alhijazi AAK, Diab S, Adam A. Optimizing tilt angles for enhanced solar PV output: A techno-environmental case study across Syrian cities. *Energy Storage and Conversion*. 2026; 4(1): 4036. <https://doi.org/10.59400/esc4036>

## ARTICLE INFO

Received: 12 February 2026

Revised: 8 March 2026

Accepted: 11 March 2026

Available online: 18 March 2026

## COPYRIGHT



Copyright © 2026 Author(s). *Energy Storage and Conversion* is published by Academic Publishing Pte. Ltd. This work is licensed under the Creative Commons Attribution (CC BY) license. <https://creativecommons.org/licenses/by/4.0/>

**Abstract:** Accurate estimation of solar radiation and optimal tilt angles is essential for maximizing the efficiency and power output of photovoltaic (PV) systems. This study investigates the optimal tilt angles and expected power generation of PV systems across major Syrian cities using climatic and geographical data. Both isotropic and anisotropic solar radiation models were evaluated, with the anisotropic model yielding approximately 5% higher energy estimates than the isotropic model. Monthly and annual optimal tilt angles were calculated using global horizontal irradiance (GHI) and ambient temperature data. The estimated total solar radiation across the studied cities reaches peak values of 8.45–8.92 kWh/m<sup>2</sup>/day in June. Using a 2.76 kWp monocrystalline silicon PV system, the predicted peak PV power output ranges from 0.92–0.96 kW during the summer months, while winter outputs decrease to approximately 0.45–0.50 kW due to reduced solar radiation and shorter daylight hours. The findings indicate that the predicted optimal tilt angle for the year is quite close to the towns' latitudes. By adjusting the photovoltaic module monthly rather than annually, it is possible to achieve a 3.8% increase in power output at ambient temperature for the investigated cities. The paper also uses geographic and meteorological data, such as monthly averages of GHI and ambient temperatures, to determine optimal tilt angles on a monthly and yearly basis. These findings highlight the significant solar energy potential across Syrian regions and provide practical guidelines for optimizing PV system installation and performance. The results can assist engineers and energy planners in improving solar energy utilization and supporting sustainable energy development in Syria.

**Keywords:** PV system efficiency; PV performance; optimal tilt angles; rated power; renewable energy systems; optimization

## 1. Introduction

In recent years, the growing focus on environmentally friendly energy approaches has, at least in part, heightened the need for research and policy on solar photovoltaic (PV) systems. A major reason for this growth is the need to replace fossil fuels with a cleaner, more plentiful, and reliable renewable alternative [1]. Unlike fossil fuels, which create environmental and geopolitical challenges, solar energy is abundant [2]. In the Middle East, solar fuels account for only 2% of the region's energy consumption and modern fossil fuels [3]. For energy-burdened solar-rich countries like Syria, developing and adopting solar photovoltaic PV technology is also critically important [4]. 98%

of the fossil fuels consumed in the Middle East have been replaced by modern solar and other renewable energy sources [5]. As of 2020, 98% of the Middle East's energy consumption was from fossil fuels, while only 2% was from renewable energy sources [6]. Fossil fuels in the Middle East accounted for 77% of energy consumption, while renewable energy sources accounted for only 23% [7]. This further signifies the integration of more renewable energy sources into the general grid [8]. By the end of 2020, 2,588 gigawatts (GW) of renewable energy capacity had been built, with 633 GW (24.5% of the total) from solar and 651 GW (25.2% of the total) from wind resources [9]. The rapid growth of photovoltaic (PV) technology over the past few decades has been driven by the need for sustainable, clean, and cost-effective energy solutions [10]. Compared with conventional energy sources, solar energy offers significant advantages, such as abundant availability, a low environmental impact, and declining installation costs. As a result, PV systems are increasingly deployed worldwide to support the transition toward low-carbon energy systems [11]. For instance, in 2020, the cost was USD 0.068 per kilowatt-hour (kWh) compared to USD 0.37 per kWh in 2010. Continued advancements in engineering and technology will likely push the levelized cost of energy further down, to a projected range of USD 0.014–0.05/kWh by 2050 [12].

Syria offers significant opportunities for renewable energy, particularly solar photovoltaics, with an average annual solar radiation of around 1,850 kWh/m<sup>2</sup> [13]. Thus, the past decade witnessed an increase in power supply to the region, primarily due to the addition of various renewable energy sources [14]. From 2011 to 2025, the region saw stellar advancements in solar power technology, and for the first time, solar power became economically feasible compared to other energy options [15]. Consequently, installed solar photovoltaic (PV) capacity is expected to grow exponentially over the next decade [16]. The recent conflicts have negatively impacted traditional energy potential and severely damaged the country's energy infrastructure, resulting in chronic power deficits and an increase in costly, polluting energy imports [17]. Decentralized, resilient, and economical solar energy systems can meet growing energy needs and enhance energy security, aiding economic development [18]. Assessing the amount of solar radiation available at any given location is important for both the design and the economic assessment of the photovoltaic system [19]. However, in many locations around the world, such as Syria, there is still very little long-term data available. Given this reality, many empirical models have been developed based on the available climate data. Many scholars have also developed models and algorithms to estimate solar radiation reaching inclined surfaces under different regions and weather conditions [20]. There are multiple determinants, including module characteristics, environmental conditions (temperature, solar radiation, and humidity), geolocation (latitude), ground reflectance, and the angle, orientation, and tilt of the solar panel, that determine the effectiveness of a photovoltaic system [21–24]. These determinants critically affect the amount of solar radiation captured by the solar panel and the functioning of the photovoltaic system, which depend on the panel orientation angle and the amount of solar radiation striking the panel [22–25]. Therefore, considering these factors facilitates the optimal installation and operation of a high-performance photovoltaic system [23–27]. Many researchers have proposed

various mathematical models and equations to determine the optimal tilt angle for maximizing the power output of a photovoltaic system [24, 28]. Furthermore, most previously published studies have been conducted for regions such as Europe, North America, and parts of Asia, while limited research has addressed PV tilt optimization for Syrian cities, despite the country's significant solar energy potential. Yadav and Chandel provided a comprehensive review of tilt angle optimization methods, but focused primarily on general modeling approaches rather than location-specific optimization [22]. Similarly, Jacobson and Jadhav estimated global optimal tilt angles using large-scale modeling; however, their analysis does not incorporate detailed local meteorological data or temperature-dependent PV performance [16]. Other studies, such as Khatib et al., analyzed tilt-angle optimization for Malaysian cities and reported that monthly adjustments can improve PV power generation by approximately 4% [10]. Likewise, Abdallah et al. evaluated optimal tilt angles for Palestine using solar radiation models, but focused primarily on radiation estimation rather than detailed PV power output analysis [17]. There is significant literature indicating that photovoltaic power output depends on the photovoltaic system tilt angle and cell temperature [29]. Although extensive research has been conducted on PV tilt optimization in many regions worldwide, few studies have examined this topic for Syrian cities, particularly considering the combined effects of solar radiation and ambient temperature on PV performance. Syria possesses substantial solar energy potential due to its favorable geographic location and high annual solar irradiance. Therefore, improving the efficiency and performance of solar PV systems is essential for enhancing energy security and promoting renewable energy adoption in the region [30]. To address this gap, this study aims to determine the optimal tilt angles for photovoltaic panels in several major Syrian cities and evaluate their impact on PV power output. The analysis incorporates geographic and meteorological data, including monthly global horizontal irradiance (GHI) and ambient temperature, to estimate solar radiation on tilted surfaces and to predict PV system performance under realistic environmental conditions [31]. In this work, both isotropic and anisotropic solar radiation models are considered to evaluate their influence on solar radiation estimation. The anisotropic model, which accounts for the non-uniform distribution of diffuse radiation, is used to calculate the monthly and annual optimal tilt angles for selected Syrian cities. The rated power of 2.76 kWp was selected based on common system capacities used in residential and small commercial photovoltaic projects in the region, as well as compatibility with the typical load profiles of similar case studies. Monocrystalline silicon technology was chosen for its higher efficiency and better performance in limited installation areas—characteristics that align with regional installation practices. In Syria and neighboring Middle Eastern countries, distributed photovoltaic systems ranging from 2.5 kWp to 5 kWp are frequently reported in grid-connected and off-grid applications, especially for residential and institutional buildings. Furthermore, a 2.76 kWp monocrystalline PV system is analyzed to estimate its potential power output under optimized tilt conditions, while accounting for the influence of PV cell temperature on system efficiency. The results aim to provide practical guidance for engineers, researchers, and policymakers involved in the planning and installation of

solar PV systems in Syria, thereby supporting the efficient utilization of the country's high solar energy potential.

## 2. Materials and methods

While many studies have investigated tilt optimization in regions such as Saudi Arabia, Malaysia, Canada, and India, there has been very limited research focusing specifically on Syria. This study provides one of the first comprehensive techno-environmental analyses of optimal PV tilt angles across multiple Syrian cities, filling a significant research gap for the region. Many previous studies focus only on solar radiation and geometric optimization of tilt angles [32]. In contrast, this research integrates ambient temperature effects into the PV power output estimation model, allowing for a more realistic evaluation of system performance under actual operating conditions. Although several studies present annual optimal tilt angles, this work provides both monthly and yearly optimal tilt values, demonstrating that monthly adjustment can increase PV output by approximately 3.8% compared to fixed annual tilt installations [33]. This provides practical guidance for improving PV system efficiency in the Syrian climate. Unlike purely geometric optimization studies, this research links solar radiation modelling, PV module temperature estimation, and power output prediction within a single framework. This integrated approach enables estimation of the actual PV power-generation potential for a 2.76 kWp system across different Syrian regions [34]. The study also highlights regional variations in solar potential across Syria, showing that inland and southern cities such as Damascus, Daraa, and Deir ez-Zur receive higher solar radiation and PV output than coastal cities like Latakia and Tartous, where humidity and cloud cover reduce irradiance. The study concentrates on optimizing solar PV tilt angles. This involves using spatial coordinates, solar radiation models, PV system performance equations, the most efficient PV panel orientations, and estimated power outputs for the chosen, unspecified Syrian cities. The primary tasks include calculating the solar angles, estimating extraterrestrial and global horizontal radiation, determining the optimal tilt angles, and predicting PV power generation. In a country such as Syria, where regions have markedly different large-scale weather systems, calculating a single average optimal tilt angle for the entire nation would be grossly unrepresentative. Considering solar radiation on an inclined surface and ambient temperature, which more conclusively determine power output, would reduce the cost of solar energy systems and energy. Research on the synergistic effect of tilt angle and ambient temperature across different locations in Syria, as well as PV array power optimization, is of great importance. The methodology consists of four main stages: (1) data collection, (2) solar radiation modelling, (3) optimal tilt angle determination, and (4) photovoltaic power output estimation.

### 2.1. Solar geometry and radiation models

Meteorological and geographical data were collected for twelve major Syrian cities, including Aleppo, Idlib, Deir ez-Zur, Hama, Homs, Damascus, Raqqa, Hasakah, Latakia, Tartous, Daraa, and Al-Suwayda. The required data included:

- Geographic coordinates (latitude and longitude);

- Monthly average global horizontal irradiance (GHI);
- Monthly average ambient temperature.

These data were obtained from publicly available climate databases such as the Climate Change Knowledge Portal and Weather Spark. The selected cities represent different climatic regions of Syria, including northern, central, coastal, and southern zones, enabling a comprehensive assessment of solar potential across the country [35]. To evaluate the influence of sky radiation modelling on photovoltaic performance estimation, two commonly used diffuse radiation models were compared in this study: the Liu and Jordan isotropic sky model and the Hay–Davies anisotropic sky model [36]. The isotropic model assumes that diffuse solar radiation is uniformly distributed across the sky dome, whereas the anisotropic model accounts for circumsolar radiation and horizon brightening effects, providing a more realistic representation of the sky radiance distribution [37]. The comparison between the two models was performed using the total solar radiation incident on the tilted surface (HT) as the primary evaluation metric [38]. Monthly and annual HT values were calculated for each selected Syrian city using both models under identical meteorological conditions. The resulting annual solar irradiation values were then used to estimate the photovoltaic power output of the 2.76 kWp PV system under consideration. The results show that the anisotropic model predicts approximately 4–5% higher annual solar energy on tilted surfaces compared with the isotropic model. This difference arises from the anisotropic model’s ability to account for directional diffuse radiation components, which increase the effective solar radiation received by tilted PV modules. The quantitative comparison between the two models is summarized in **Table 1**.

**Table 1.** The quantitative comparison between the Liu and Jordan, and Hay–Davies models.

Model	Radiation model type	Annual HT (kWh/m <sup>2</sup> /year)	Estimated PV output (kWh/year)	Difference
Liu and Jordan	Isotropic	2,115	3,680	-
Hay–Davies	Anisotropic	2,210	3,825	+4.5%

Maximizing energy returns and economic feasibility relies on improving the performance of solar PV systems. One of the main components affecting the efficiency and performance of PV systems is the solar panels’ tilt angle [39]. The optimal tilt angle, positioning the solar panels at the ideal location, will guarantee that the panels receive the maximum solar radiation for the entire day and all the seasons of the year. The optimal angle is dynamic and depends on latitude and the time of year because of the sun’s changing position [40]. Hence, to gain the maximum possible power generation, trying to establish the ideal tilt angle for the location in question is critical. Apart from the diffuse sky radiation element, which can be segregated into isotropic and anisotropic models, there exist mathematical descriptions of the solar radiation model that are similar to one another. Isotropic diffuse models are solely intensity and radiation-based. In contrast to this, anisotropic models consider the circumsolar diffuse and/or the horizontal-brightening components on an inclined surface. The ability to accurately determine the solar radiation that will be incident on the PV panel hinges on the accuracy of the calculations of the solar angles [41]. Important solar angles

include declination angle ( $\delta$ ), which pertains to the Earth's tilt relative to its orbital plane, and hour angle ( $\omega$ ), which represents the position of the sun with respect to the local meridian, as determined by (1).

$$\delta = 23.45 * \sin \left( \frac{360}{365} (284 + N) \right) \quad (1)$$

Let  $N$  denote the day of the year. These angles are obtained for the midpoints of each month, in order to signify the monthly average relative positions of the sun. The calculation of the sunset hour angle ( $\omega_{ss}$ ) is essential for determining the calculation of the total daylight hours and the extraterrestrial radiation. It is also calculated based on the geographic latitude of the city and the declination angle.

$$\omega_{ss} = \min \begin{cases} \cos^{-1} (-\tan \varphi * \tan \delta) \\ \cos^{-1} (-\tan (\varphi - \beta) * \tan \delta) \end{cases} \quad (2)$$

Here,  $\varphi$  designates the latitude of the location and  $\beta$  represents the angle of the slope between the surface and the plane. Extraterrestrial radiation ( $H_o$ ), which refers to solar radiation recorded on a horizontal surface before it meets the Earth's atmosphere, can be determined using a specific equation that uses the solar constant, the applicable day of the year, latitude, declination angle, and sunset hour angle. To find the monthly average daily extraterrestrial radiation ( $H_o$ ), one calculates the integrated value of (1) over the course of the day. Thus,  $H_o$  can be determined as (3).

$$H_o = \frac{24 \times 3,600 \times G_{sc}}{\pi} \left( 1 + 0.033 \cos \frac{360N}{365} \right) \left( \frac{\pi \omega_{ss}}{180} \sin \varphi \sin \delta + \cos \varphi \cos \delta \sin \omega_{ss} \right) \quad (3)$$

Because the value for GSC Solar Constant is  $\sim 1,367 \text{ W/m}^2$ ,  $H_o$  is expressed in  $\text{J/m}^2/\text{day}$ . This is the value used to conduct the evaluation for atmosphere attenuation. After that, the clearness index ( $K_T$ ) is determined by analysing the difference between the calculated extraterrestrial radiation and the monthly average global horizontal irradiance (GHI), which is obtained from Weather Spark data. This index serves to quantify the fraction of solar radiation that is transmitted through the atmosphere and reaches the surface of the Earth. For calculating the diffuse component of solar radiation, the diffuse fraction (where  $K_T$  is the average clearness index) is approximated using equations that connect it to the clearness index and the sunset hour angle. The monthly average clearness index ( $K_T$ ) is defined as the ratio of average daily global radiation at the ground ( $H$ ) and average daily extraterrestrial radiation ( $H_o$ ) (i.e., solar radiation at the top of the atmosphere). Thus,  $K_T$  can be calculated as (4).

$$K_T = \frac{H}{H_o} \quad (4)$$

Equations (5) and (6) provide the ratio of average daily diffuse radiation on a horizontal surface ( $H_d$ ) to the average daily global radiation at the ground ( $H$ ). To derive Equations (5) and (6), the sunset hour angle criterion ( $\omega_{ss}$ ) is used to select the correct polynomial, which effectively addresses the seasonal and latitudinal distributions. In case (a), ( $\omega_{ss} \leq 81.4^\circ$ ) is considered, which is applied to shorter days, typically in winter months and at higher latitudes.

$$\frac{H_d}{H} = 1.391 - 3.560K_T + 4.189K_T^2 - 2.137K_T^3 \quad (5)$$

Case (b) is ( $\omega_{ss} > 81.4^\circ$ ), where is applied to longer days (typically summer months or lower latitudes)

$$\frac{H_d}{H} = 1.311 - 3.022K_T + 3.427K_T^2 - 1.821K_T^3 \quad (6)$$

The average clearness index values between 0.3 and 0.8 apply to both equations. The most commonly measured total solar radiation and the day length can be used in Equations (5) and (6) to make a prediction about the average daily diffuse solar radiation. Energy simulation, system performance modelling, and solar resource assessment all require the use of Equations (5) and (6), and many other tasks and projects.

$$H_T = H_d R_d + (H_g - H_d) R_b + H_g \rho_g \left( \frac{1 - \cos \beta}{2} \right) \quad (7)$$

$H_d$  = fraction of diffuse monthly radiation.  $H$  = global horizontal surface radiation. Horizontal global surface radiation is defined by  $H_g$ . Equations (8) and (9) define the average daily beam and diffuse radiation on a tilted surface,  $R_b$  and  $R_d$ .  $R_b$  is the ratio of the incidence angle cosine and the cosine of the zenith angle.

$$R_b = \frac{\sin(\varphi - \beta) \times \sin(\delta) + \cos(\varphi - \beta) \times \cos(\delta) \times \cos(\omega_{ss})}{\sin(\varphi) \times \sin(\delta) + \cos(\varphi) \times \cos(\delta) \times \cos(\omega_{ss})} \quad (8)$$

$$R_d = \frac{3 + \cos(2\beta)}{4} \quad (9)$$

This study was able to make certain approximations primarily because of a lack of extensive data and reliance on typical ranges of the clearness index. Ideally, more atmospheric data would be available to more accurately diffuse radiation. This is due to the need for more detailed atmospheric data in order to quantitatively diffuse radiation more accurately.

## 2.2. Optimal tilt angle determination

Total solar radiation incident on a tilted surface ( $H_T$ ) consists of three components: beam, diffuse, and ground-reflected radiation. In order to compute these components on a tilted surface, two main ratios must be defined. The first is the Ratio of beam radiation ( $R_b$ ): This ratio measures the difference in intensity of beam radiation between a horizontal surface and a tilted surface. It is defined using latitude, tilt angle, declination angle, and the hour angle. For simplification purposes in calculating the optimal tilt for any given month,  $R_b$  was determined for solar noon (hour angle = 0). The other is the Ratio of diffuse radiation ( $R_d$ ): This ratio measures the diffuse radiation value received on the tilted surface. Due to constraints of the data, the Liu and Jordan diffusely illuminated isotropic sky model was used to compute  $R_d$ . The model significantly simplifies the computation based on the tilt angle, which assumes diffuse radiation is equally distributed across the sky. Finally, the total solar radiation ( $H_T$ ) on a tilted surface is calculated by the following Equation (10),

$$H_T = H_g \left[ \left(1 - \frac{H_d}{H_g}\right) * R_b + \frac{H_d}{H_g} * R_d + \rho_g \frac{1 - \cos \beta}{2} \right] \quad (10)$$

where:

$H_T$  is the total solar irradiance on a tilted surface ( $\text{W/m}^2$  or  $\text{kWh/m}^2$ ).  $H_g$  is global horizontal irradiance, which is the total solar radiation received on a horizontal surface.  $H_d$  is the diffuse horizontal irradiance, which is the scattered component of  $H_g$ .  $\frac{H_d}{H_g}$  is the fraction of global radiation that is diffuse.  $\left(1 - \frac{H_d}{H_g}\right)$  is the fraction of global radiation that is beam (direct).  $R_b$  is the ratio of the beam radiation on the tilted surface to that on a horizontal surface. This is a geometric factor depending on the position of the sun and the surface tilt.  $R_d$  is the ratio of diffuse radiation on the tilted surface to that on a horizontal surface. For an isotropic sky, it is often modelled as  $\frac{1 + \cos \beta}{2}$ .  $\rho_g$  is ground albedo (reflectivity), which is between 0.1 (dark) and 0.7 (snow). In this study, a constant value of ( $\rho_g = 0.2$ ) was adopted for all analyzed cities.  $\beta$  is the tilt angle of the surface from horizontal.  $\frac{1 - \cos \beta}{2}$  is the view factor from the surface to the ground, and it represents the fraction of the hemisphere that is “seen” by the surface, which is the ground. For a specific month, the optimal tilt angle is obtained by iterating through each angle of  $0^\circ$  to  $90^\circ$ , then selecting the angle that maximizes the calculated total solar radiation ( $H_T$ ) on the PV panel. This is achieved by calculating the monthly  $H_T$  sums for each fixed tilt angle and determining which angle has the maximum annual total.

### 2.3. PV power output estimation

It should be noted that the PV power output values reported in this study represent the estimated instantaneous output power under the monthly average peak irradiance conditions, rather than the rated output of the system under Standard Test Conditions (STC). The values shown in the results correspond to the calculated power at representative peak irradiance periods using monthly averaged solar radiation data. Since the model uses monthly average global horizontal irradiance and ambient temperature rather than instantaneous irradiance at STC ( $1,000 \text{ W/m}^2$  and  $25^\circ\text{C}$ ), the resulting PV output values represent typical peak operating power during that month rather than the nominal rated power of the system. Furthermore, the predicted PV power output remains below the rated capacity of 2.76 kWp because real operating conditions differ from Standard Test Conditions. In particular, the incident irradiance on the tilted surface (GT) is often lower than the STC reference value of  $1,000 \text{ W/m}^2$ , and the PV cell temperature typically exceeds the standard temperature of  $25^\circ\text{C}$ . The negative temperature coefficient of power results in a reduction in module efficiency as the cell temperature increases. Additional factors such as atmospheric attenuation, diffuse radiation components, and the use of monthly averaged climatic data also contribute to lower estimated power outputs compared with the nominal system rating.

The photovoltaic power output was estimated using a simplified performance model that considers the influence of solar irradiance and cell temperature on PV efficiency. A model that factors in ambient temperature and the solar radiation impinging on the PV surface is used to compute the PV cell temperature ( $T_C$ ). Equation

(11) defines the relationship among cell temperature, ambient temperature, nominal operating cell temperature (*NOCT*), conditions and incident solar radiation. Adopted from the original study are the *NOCT* conditions ( $G_{T,NOCT} = 800 \text{ W/m}^2$ ,  $T_{a,NOCT} = 20 \text{ }^\circ\text{C}$ ,  $T_{c,NOCT} = 47 \text{ }^\circ\text{C}$ ) and PV module characteristics ( $\alpha_P = -0.0046$ ,  $\eta_{mp,STC} = 0.135$ ,  $\tau = 0.9$ ,  $\alpha = 0.9$ ).

$$T_C = \frac{T_a + (T_{c,NOCT} - T_{a,NOCT})\left(\frac{G_T}{G_{T,NOCT}}\right)\left(1 - \frac{\eta_{mp,STC}(1 - \alpha_P T_{c,STC})}{\tau \alpha}\right)}{1 + (T_{c,NOCT} - T_{a,NOCT})\left(\frac{G_T}{G_{T,NOCT}}\right)\left(\frac{\alpha_P T_{c,STC}}{\tau \alpha}\right)} \quad (11)$$

PV power output ( $P_{pv}$ ) is predicted from a simplified model that incorporates the rated power of the PV system, the cell temperature, and the actual solar radiation on the tilted surface. Consistent with the original study, the rated power of the PV system was assumed to be 2.76 kWp at Standard Test Conditions (STC: 1,000 W/m<sup>2</sup> irradiance, 25 °C cell temperature). The power output is calculated in Equation (12).

$$P_{pv} = P_{rated} \left( \frac{G_T}{G_{STC}} \right) (1 + \gamma (T_C - T_{STC})) \quad (12)$$

Where,  $P_{pv}$ : The expected power output of the PV system under real-world conditions. This is the value you are calculating.  $P_{rated}$ : The “nameplate” power of the system under ideal laboratory conditions, known as Standard Test Conditions (STC),  $P_{pv} = 2.76 \text{ kWp}$ .  $\frac{G_T}{G_{STC}}$ : ratio adjusts the rated power for the actual available sunlight.  $G_T$ : The real-world solar irradiance incident on the PV panels.  $G_{STC}$ : The irradiance at STC, which is a constant 1,000 W/m<sup>2</sup>.  $\gamma (T_C - T_{STC})$  factor adjusts the power for the efficiency loss (or gain) due to the cell temperature deviating from the standard.  $\gamma$ : The temperature coefficient of power. It indicates how much the power changes per degree Celsius ( $\gamma = -0.0046 \text{ }^\circ\text{C}^{-1}$ ). This negative value is typical for silicon solar cells and means that for every 1 °C the cell temperature is above 25 °C, the power output decreases by 0.46%.  $T_C$ : The calculated real-world operating temperature of the PV cells.  $T_{STC}$ : The cell temperature at STC, which is a constant 25 °C. This model allows the estimation of real-world PV output by accounting for temperature-related efficiency losses.

#### 2.4. PV cell single diode model

To estimate the maximum power produced by a tilted solar PV array, we began by running simulations in MATLAB (MATrix LABoratory). **Figure 1** shows a flowchart for optimizing the tilt angle to maximize power generation from a PV array. The first step consists of obtaining latitude ( $\phi$ ), ambient air temperature ( $T_a$ ), monthly average daily solar radiation ( $H_g$ ), and the day of the year ( $n$ ) for the selected location. After the area was selected, the declination angle ( $\delta$ ), incident angle ( $\theta$ ), and sunset hour angle ( $\omega_{ss}$ ) were determined, followed by the calculation of the clearness index ( $K_T$ ) and extraterrestrial radiation. Ho for all 365 days of the year has been calculated using the above parameters.

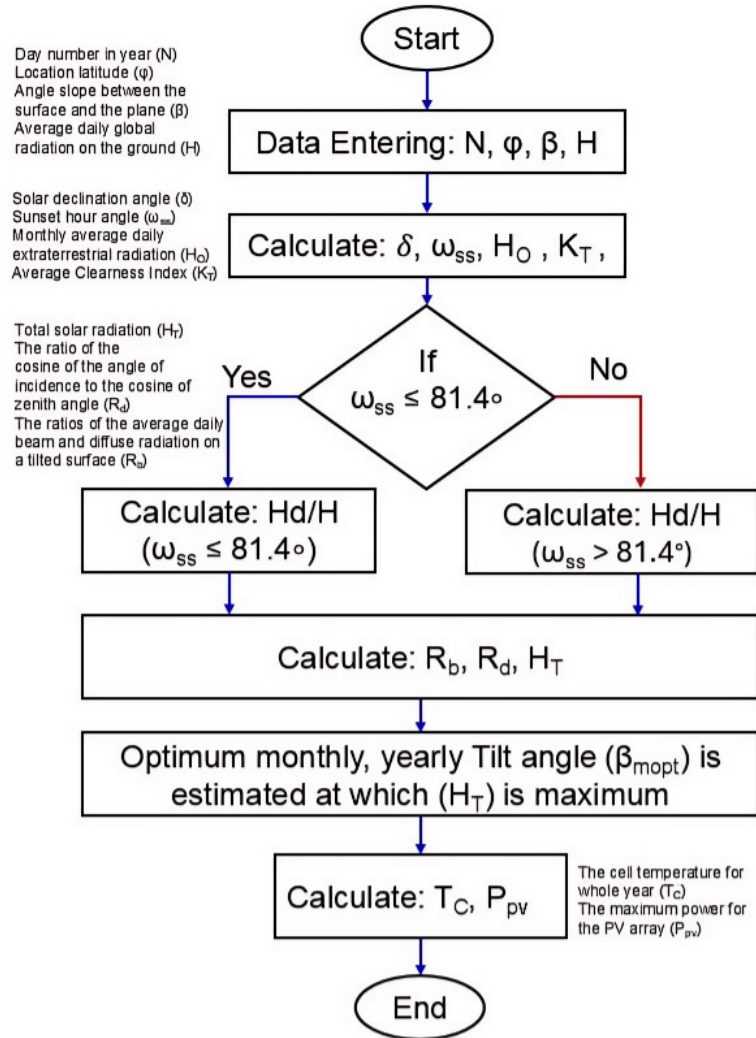


**Figure 1.** Flowchart of optimizing the tilt angle to generate maximum power from the PV array.

All the above parameters shall be calculated for a range of slope values ( $\beta$ ) ranging from 0 to 90. A decision block decides whether the sunset hour angle ( $\omega_{ss} \leq 81.4$ ) is satisfied or not, and based on this condition, the monthly diffuse fraction is calculated using two equations described in (5) and (6). To obtain the optimum tilt angle, the total solar radiation ( $H_T$ ) hitting the surface is calculated for varying tilt angles ( $\beta$ ) throughout the year. The optimum tilt angle for each day is estimated by searching for slope values at which the maximum total solar radiation is achieved.

## 2.5. Data collection

Monthly average global horizontal irradiance (GHI) and ambient temperature data for Syrian cities were collected from the Climate Change Knowledge Portal. Syria is characterized by the corresponding average value of solar energy falling on a horizontal surface [ $\text{kWh/m}^2/\text{year}$ ], where main cities like Latakia, Tartous, Hasakah, Raqqa, Aleppo, Deir ez-Zor, Idlib, Hama, Homs, Damascus, Daraa, and Al-Suwayda are shown in **Figure 2**. Geographical coordinates (latitude and longitude) for each city were also obtained from the same source. This data forms the basis for all subsequent calculations and analyses.

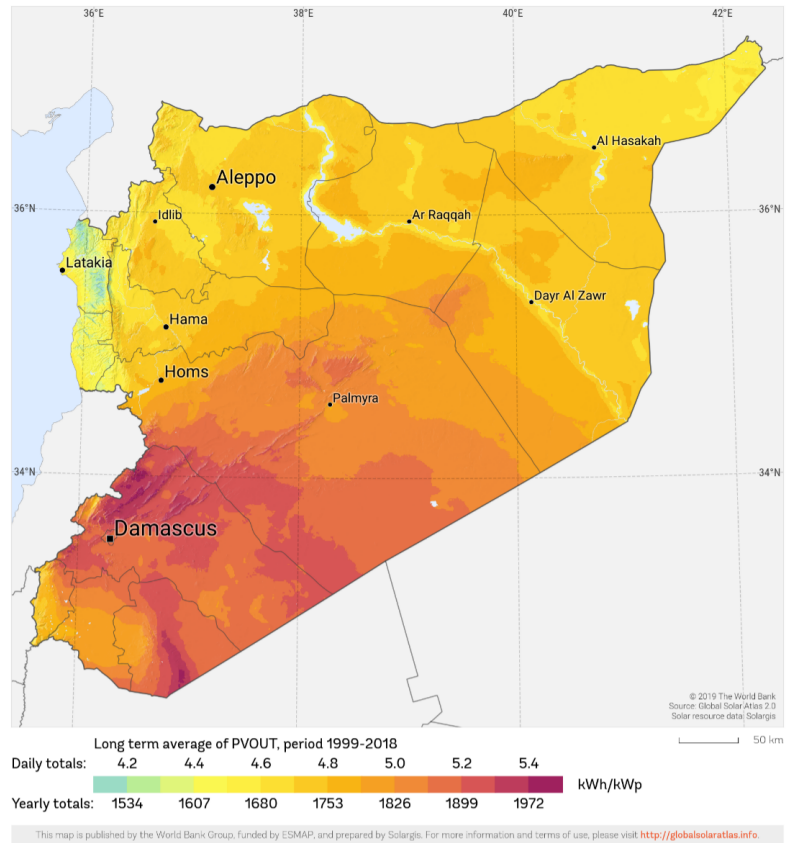


**Figure 2.** The average value of solar energy falling on a horizontal surface [ $\text{kWh}/\text{m}^2/\text{year}$ ].

The entire analysis process was implemented using MATLAB. The simulation algorithm calculated solar geometry parameters for each day of the year, estimated radiation components, and iteratively evaluated total solar radiation for tilt angles ranging from  $0^\circ$  to  $90^\circ$ . The optimal tilt angles were determined by identifying the angles that maximize the total incident solar radiation. Finally, the optimized radiation values were used to estimate the PV power output for each city. The methodology enables a comparative assessment of solar potential across different regions of Syria while identifying optimal panel orientations for improved photovoltaic performance.

## 2.6. Error analysis of the simplified diffuse radiation model

The diffuse radiation component in this study was estimated using the simplified isotropic sky assumption proposed by Liu and Jordan. Although this approach is widely used due to its computational simplicity and limited data requirements, it may introduce deviations compared with more advanced anisotropic sky models that account for circumsolar brightening and horizon effects. To evaluate the accuracy of the simplified approach, the obtained results were compared with findings reported in the literature using anisotropic models such as the Hay–Davies and Perez models. Previous comparative studies indicate that isotropic models typically underestimate the diffuse radiation component on tilted surfaces by approximately 3–7%, depending on atmospheric conditions and seasonal variations. As a result, the total solar radiation incident on tilted surfaces may differ by approximately 2–5% when compared with anisotropic formulations. In the context of the present analysis, this deviation produces only a minor variation in the calculated optimal tilt angles. Sensitivity analysis

shows that a 5% variation in the diffuse radiation component changes the estimated optimal tilt angle by approximately  $\pm 1^\circ$  to  $\pm 2^\circ$  and affects the predicted PV power output by less than 4%. Therefore, the simplified model provides sufficiently accurate results for comparative evaluation of tilt angles across different Syrian cities while maintaining computational efficiency. Despite these acceptable deviations, the use of advanced anisotropic diffuse radiation models may further improve prediction accuracy, particularly in locations with high atmospheric turbidity or significant cloud scattering. Future work may incorporate high-resolution meteorological datasets and advanced models such as the Perez diffuse model to refine the estimation of solar radiation on inclined surfaces.

### 3. Experiment, results, and discussion

The findings for all Syrian cities, including the optimal monthly and yearly tilt angles, total solar irradiance on the tilted plane, and estimated photovoltaic power output, are sequentially covered in this section. The specific geographical and climatic characteristics of each city are taken into account when discussing the results.

Damascus, the capital city, is located at approximately  $33.5^\circ$  N latitude. Damascus shows optimal tilt angles ranging from  $55^\circ$  in December to  $10^\circ$  in June. The highest total solar radiation and PV power output are observed in June ( $8.92 \text{ kWh/m}^2/\text{day}$  and  $0.96 \text{ kW}$ , respectively). The annual optimal tilt angle for Damascus is  $31^\circ$ , reflecting its more southerly latitude and generally higher solar irradiance.

At a latitude of about  $36.2^\circ$  N, Aleppo has a high degree of variability in solar radiation as well as substantial seasonal variation in temperature. Throughout the winter months, the optimal tilt angle remains a steep  $56^\circ$ , which progresses through the warmer months to a shallow  $13^\circ$  in June. July is the peak summer month, and as expected, the total solar radiation is also highest in this month at  $8.63 \text{ kWh/m}^2/\text{day}$ . The estimated photovoltaic power output trends similarly to the power output, which reaches a maximum of  $0.92 \text{ kW}$  in June and a minimum of  $0.45 \text{ kW}$  in December. An optimal yearly tilt angle of  $34^\circ$  was calculated as the most advantageous position for all seasons to provide the best overall performance for Aleppo.

Deir ez-Zur has a latitude of approximately  $35.3^\circ$  N. Deir ez-Zur has a hot desert climate and also receives a substantial amount of solar radiation. For Deir ez-Zur, the optimal solar panel tilt angles are  $56$  degrees in December and  $12$  degrees in June. This city receives the most solar radiation in June ( $8.66 \text{ kWh/m}^2/\text{day}$ ), so the peak PV power output is  $0.91 \text{ kW}$  during this month. Deir ez-Zur has an optimal annual tilt of  $33^\circ$ , which is slightly less than Aleppo, where the latitude is further north.

Idlib is located at approximately  $35.9^\circ$  N latitude. This area has similar solar characteristics to Aleppo due to their comparable geographical positions. For Idlib, the optimal tilt angles are  $56^\circ$  and  $13^\circ$  in June. This aligns with the solar radiation, as the peak solar radiation occurs in June ( $8.57 \text{ kWh/m}^2/\text{day}$ ), and the power output also stands at  $0.93 \text{ kW}$ . The annual optimal tilt angle for Idlib is  $34^\circ$ , which is expected based on its latitude due to its similarity with Aleppo.

As is the case with latitude  $35.1^\circ$  N locations, Hama also has a marked seasonal variation with values of optimal tilt angles and PV performance. For Hama, these

optimal tilt angles vary from  $56^\circ$  in December to  $12^\circ$  in June. June yields peak total solar radiation and PV power output, at  $8.65 \text{ kWh/m}^2/\text{day}$  and  $0.93 \text{ kW}$ . Hama's annual optimal tilt angle is  $33^\circ$  and correlates with Hama's latitude and is consistent with the overall collection of data for the other Hama cities in the north of Syria.

At a latitude of  $34.7^\circ \text{ N}$ , the PV performance and optimal tilt angle patterns for Homs follow the same trend as other cities in the centre of Syria. Homs also has optimal tilt angles from  $56^\circ$  in December to  $12^\circ$  in June. Again, the highest total solar radiation and PV power output are in June, for the values of  $8.74 \text{ kWh/m}^2/\text{day}$  and  $0.94 \text{ kW}$ . As for Homs, the annual optimal tilt angle of  $32^\circ$  is a reflection of its position relative to Aleppo and Idlib, which is latitude-wise, the most southerly.

Latakia, at approximately  $35.5^\circ \text{ N}$ , shows clear seasonal variation for both the optimal tilt angles and PV performance. There, the optimal tilt angles from Latakia stretch from  $56^\circ$  in December to  $12^\circ$  in June. June has the highest total solar radiation and PV power output for the month at  $8.45 \text{ kWh/m}^2/\text{day}$  and  $0.93 \text{ kW}$ , respectively. The annual optimal tilt for Latakia is  $30^\circ$ , reflecting  $30^\circ$  latitude globally and consistent with the expected trend for other northern Syrian cities.

Tartous is located at  $34.9^\circ \text{ N}$  latitude and is similar to Latakia in that it also shows clear seasonal variations for optimal tilt angles and PV performance. In Tartous, optimal tilt angles for Tartous stretch from  $55^\circ$  in December to  $12^\circ$  in June. For June, the total solar radiation and PV power output are exceptional at  $8.54 \text{ kWh/m}^2/\text{day}$  and  $0.93 \text{ kW}$  for the month. The annual optimal tilt for Tartous is  $29^\circ$ , reflecting  $29^\circ$  latitude globally and consistent with the expected trend for other northern Syrian cities.

The analysis considers Hasakah's latitude of  $36.47^\circ \text{ N}$ . Hasakah's optimal angles are  $57^\circ$  in December and  $13^\circ$  in June. From June to September, there is a significant increase in total solar radiation ( $8.69 \text{ kWh/m}^2/\text{day}$ ) and PV power output ( $0.92 \text{ kW}$ ), making June the best month for solar radiation and PV output. Annual optimal PV power output for Hasakah is  $0.31 \text{ kW}$ . Annual optimal tilt of  $31^\circ$  is consistent with Hasakah's latitude and is in line with the rest of the northern cities in Syria.

Hasakah ( $36.47^\circ \text{ N}$ ) exhibits notable seasonal changes in optimal tilt angles and PV performance. From December to June, optimal tilt angles change from  $57^\circ$  to  $13^\circ$ , respectively. June also displays the highest total solar radiation and PV power output ( $8.69 \text{ kWh/m}^2/\text{day}$  and  $0.92 \text{ kW}$ ). The annual optimal tilt angle averages  $31^\circ$ , showing consistency with other northern Syrian cities and Hasakah's geographical position.

Raqqa ( $35.95^\circ \text{ N}$ ) also has seasonal changes in optimal tilt angles and PV performance. From December to June, optimal tilt angles change from  $56^\circ$  to  $13^\circ$ , respectively. June sees the highest total solar radiation and PV power output ( $8.67 \text{ kWh/m}^2/\text{day}$  and  $0.92 \text{ kW}$ ). The annual optimal tilt angle is  $31^\circ$  and is in line with the general trend in other northern Syrian cities.

Al-Suwayda exhibits significant spatial variation for both optimal tilt angles for photovoltaic (PV) systems and the performance of the PV system at various angles. The angles required for the optimal azimuthal and protective tilt at PV in Al-Suwayda are the most extreme in Syria, being  $54^\circ$  and  $10^\circ$  for the months of December and June, specifically pertaining to the months of PV performance variation. Al-Suwayda experiences the most extreme tilt angles for optimal PV tilt

adjustment, indicating that throughout the year, Al-Suwayda's azimuthal seasonal PV tilt adjustment shows the greatest variation. This suggests that, compared to Daraa, Al-Suwayda experiences the most significant increase in azimuthal PV performance. Al-Suwayda also displays the most extreme azimuth optimal value of  $28^\circ$ , further supporting the hypothesis that Daraa and Al-Suwayda reflect a general trend in solar PV performance in southwestern Syria. The differences observed in Al-Suwayda are minimal yet significant, demonstrating that the general spatial performance trend varies from all perspectives.

Daraa shows the most southerly solar characteristics in comparison to the other cities in the study. For Daraa, the optimal tilt angles range from  $54^\circ$  in December to  $10^\circ$  in June. The highest total solar radiation and PV power output are recorded in June (8.80 kWh/m<sup>2</sup>/day and 0.94 kW, respectively). This indicates that Daraa most likely possesses the optimal climatic conditions in the study. The annual optimal tilt angle for Daraa is  $30^\circ$ , which is the lowest among the studied cities, consistent with its most southerly latitude.

There is a strong correlation between each city's latitude and its annual optimal tilt angle, confirming the empirical relationship where the optimal annual tilt angle roughly equals the location's latitude  $\pm$  a few degrees based on local climatic factors. Latitude–tilt angle relationship is shown in **Table 2**.

**Table 2.** Latitude–tilt angle relationship.

Region	Approx. latitude ( $^\circ$ N)	Annual optimal tilt ( $^\circ$ )	Trend
Northern Syria (Aleppo, Idlib, Hasakah, Raqqa)	35.5–36.5	31–34	Slightly higher tilt angles
Central Syria (Hama, Homs, Deir ez-Zur)	34–35	32–33	Moderate tilt angles
Western Coastal (Latakia, Tartous)	34.5–35.5	29–30	Lower tilt due to maritime climate
Southern Syria (Damascus, Daraa, Al-Suwayda)	32–33.5	28–31	Lowest tilt angles

The highest values of solar radiation received in all cities lie in the range of 8.45–8.92 kWh/m<sup>2</sup>/day, and total potential PV system outputs range from 0.91–0.96 kW during the month of June. Damascus obtains the highest solar radiation (8.92 kWh/m<sup>2</sup>/day) as well as PV output (0.96 kW) due to its prominent solar potential. Meanwhile, Latakia has the lowest solar radiation (8.45 kWh/m<sup>2</sup>/day), which can be attributed to the maritime humidity and cloud cover of the Mediterranean. This implies that coastal climates tend to have slightly lower solar gain compared to the inland desert and semi-arid regions. **Figure 3** displays the maximum total solar radiation in kWh/m<sup>2</sup>/day across Syrian cities. The climatic conditions across different regions of the country significantly impact solar performance. Deir ez-Zur, Raqqa, and Hasakah, as desert and semi-arid cities, benefit from high solar radiation levels due to the prevalence of clear and uncluttered skies. On the other hand, cities like Latakia and Tartous have some radiation losses due to more humidity and sporadic cloud cover, which leads to somewhat more condensation and precipitation. Southern highland cities (Daraa, Al-Suwayda) combine strong irradiance with moderate temperatures, yielding high PV efficiency. PV Cell Temperature ( $^\circ$ C) for Syrian cities is shown in **Figure 4**. The PV power output mirrors the trends in radiation. Peak outputs of 0.92–0.96 kW are achieved in June and July. The outputs observed are lowest in December,

approximately 0.45–0.5 kW, considering the factors of reduced solar intensity and the presence of shorter daylight hours. Considering the seasonal differences, solar energy generation capacity differs by around 50% in the winter and summer months. This shows the importance of optimal tilt adjustment, or the use of tracking systems, in order to capture higher solar energy and boost solar energy performance throughout the year.

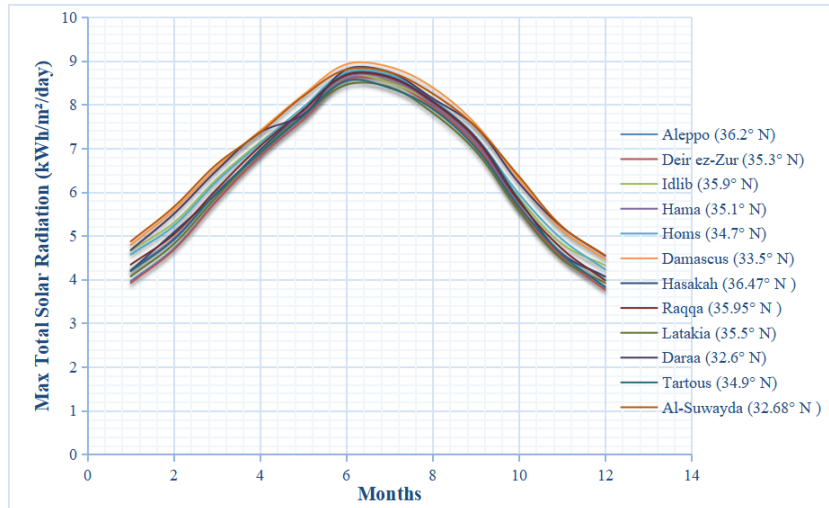


**Figure 3.** Max total solar radiation (kWh/m<sup>2</sup>/day) for Syrian cities.

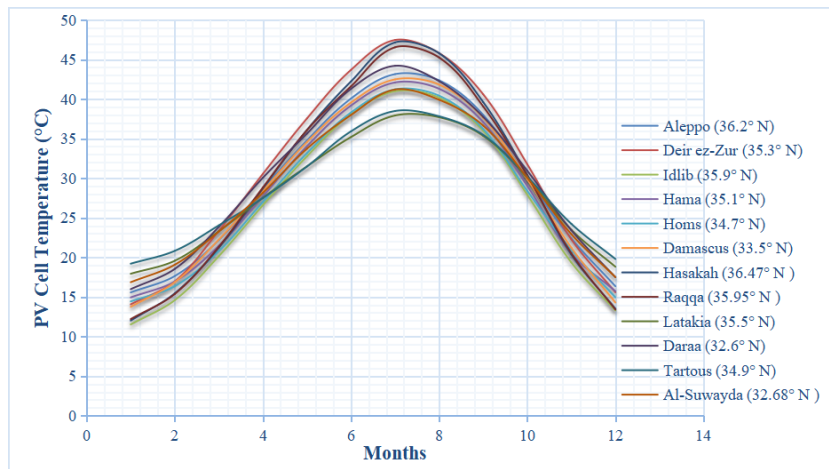


**Figure 4.** PV cell temperature (°C) for Syrian cities.

PV Power Output (kW) for Syrian cities is shown in **Figure 5**. The symmetrical nature of the findings is confirmed by the fact that the optimal annual tilt angles (28–34°) are in close alignment with the geographical coordinates of Syria (32–37° N). Data indicates that the southern and inland regions of Syria experience the highest levels of solar radiation and PV system efficiency, implying that these regions are the most favourable for large-scale PV system installations. Coastal region installations still require slightly larger systems or include tracking systems due to lower levels of irradiance. The pronounced seasonal differences of solar radiation received demonstrate the benefit of adjustable tilt systems, thus further confirming results in **Figure 6**, Optimal tilt angle (°) Syria. The PV power output values reported in this section correspond to the estimated instantaneous peak power under monthly average irradiance and temperature conditions for a 2.76 kWp PV system. These

values should not be interpreted as the system’s rated output under Standard Test Conditions (STC). Instead, they represent typical operating power levels calculated from the real environmental conditions for each city. The peak values observed in the results (approximately 0.92–0.96 kW in June) are lower than the rated system capacity because the simulations are based on average meteorological data and account for temperature-related efficiency losses. Under actual instantaneous high-irradiance conditions close to 1,000 W/m<sup>2</sup> and lower cell temperatures, the PV system could approach its rated capacity.

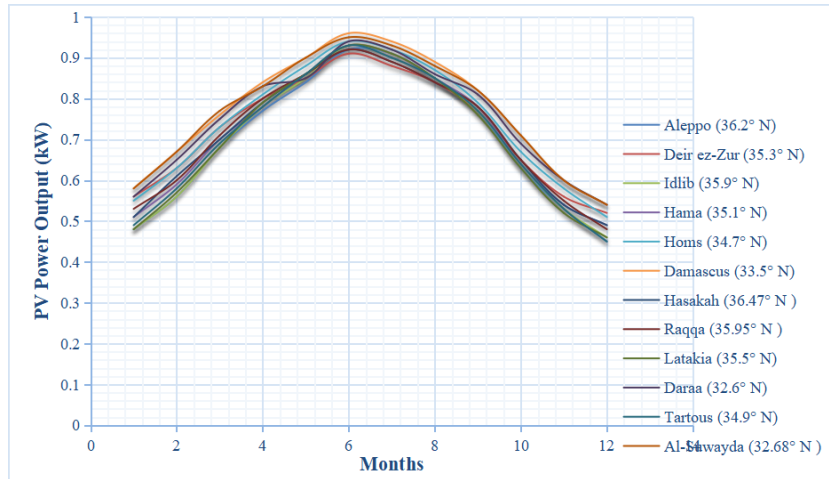


**Figure 5.** PV power output (kW) for Syrian cities.

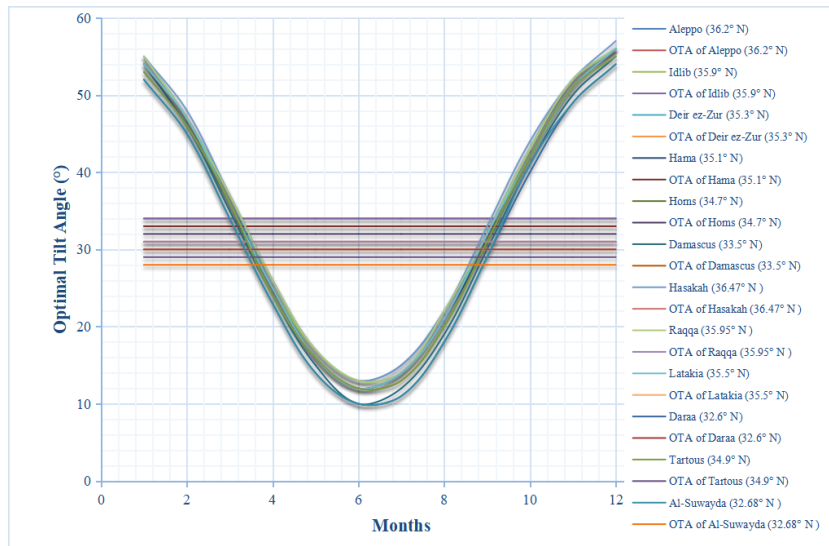


**Figure 6.** Optimal tilt angle (°) for Syrian cities.

This analysis affirms the significant potential for solar energy in all parts of Syria. Optimal tilt angles and performance metrics remain constant, varying primarily with latitude and climatic differences. Cities in the south and the interior, particularly Damascus, Daraa, and Deir ez-Zur, stand out for their maximum potential solar energy output and are the first candidates for PV system implementation. Coastal and northern regions still provide viable conditions but may require optimized panel configurations for maximum efficiency.

## 4. Conclusion

This study investigated the optimal tilt angles and photovoltaic (PV) performance across major Syrian cities by incorporating solar radiation models, geographic coordinates, and ambient temperature data. The results indicate that the optimal annual tilt angles for PV installations in Syria closely correspond to the geographic latitude of each location, ranging from 28° to 34°. Specifically, optimal annual tilt angles were calculated as 34° for Aleppo and Idlib, 33° for Deir ez-Zur and Hama, 32° for Homs, 31° for Damascus, Hasakah, and Raqqa, 30° for Latakia and Daraa, 29° for Tartous, and 28° for Al-Suwayda. Seasonal analysis shows significant variation in optimal tilt angles, ranging from approximately 54–57° during winter months to 10–13° during summer months. These seasonal variations reflect the changing solar altitude throughout the year and highlight the importance of proper panel orientation for maximizing solar radiation capture. The analysis also demonstrated that solar radiation values across Syrian cities reach peak levels of approximately 8.45–8.92 kWh/m<sup>2</sup>/day during the summer months. Under these conditions, the simulated 2.76 kWp photovoltaic system produced peak power outputs ranging between 0.92 kW and 0.96 kW, with the highest output recorded in Damascus. Conversely, winter months exhibited lower solar radiation and reduced PV output, with power levels decreasing to approximately 0.45–0.50 kW due to shorter daylight hours and lower solar intensity. Furthermore, the comparison between radiation models revealed that anisotropic models can estimate approximately 5% higher energy output compared to isotropic models. The results also indicate that adjusting the PV tilt angle monthly rather than maintaining a fixed annual tilt can increase annual energy production by approximately 3.8%. The findings of this study highlight the significant solar energy potential available across Syria and emphasize the importance of optimizing PV panel orientation to maximize system efficiency. The results provide practical guidance for engineers, policymakers, and renewable energy planners involved in the design and installation of solar photovoltaic systems. In particular, the identified optimal tilt angles can assist in improving system performance, reducing energy losses, and increasing the economic feasibility of solar energy projects across different regions of the country. From a practical perspective, the outcomes of this research can support the development of decentralized solar energy systems, rooftop PV installations, and solar-powered irrigation or water pumping applications, which are particularly valuable for regions experiencing energy shortages. Optimizing PV installations using the recommended tilt angles can contribute to improved energy security and sustainable electricity generation in Syria. Future research should extend this work by incorporating additional real-world factors such as dust accumulation, shading effects, wind cooling, and long-term system degradation, which can significantly influence PV performance in desert and semi-arid climates. Moreover, future studies could employ high-resolution hourly meteorological data and advanced anisotropic radiation models to further improve the accuracy of solar radiation estimation. Economic analysis, including installation costs and the feasibility of tracking systems, would also be beneficial for evaluating the practical implementation of optimized PV systems in

different regions. Such investigations would provide deeper insights and contribute to the continued advancement of solar energy deployment in Syria and similar climates worldwide.

## Abbreviation

<b>Symbol</b>	<b>Description</b>	<b>Unit</b>
$N$	Day number of the year	–
$\delta$	Solar declination angle	degree (°)
$\omega$	Hour angle	degree (°)
$\omega_{ss}$	Sunset hour angle	degree (°)
$\varphi$	Latitude of the location	degree (°)
$\beta$	Tilt angle of the PV panel relative to the horizontal surface	degree (°)
$H_o$	Extraterrestrial solar radiation on a horizontal surface	kWh/m <sup>2</sup> /day
$H$	Monthly average daily global solar radiation on a horizontal surface	kWh/m <sup>2</sup> /day
$H_g$	Global horizontal irradiance	kWh/m <sup>2</sup> /day
$H_d$	Diffuse solar radiation on a horizontal surface	kWh/m <sup>2</sup> /day
$H_T$	Total solar radiation incident on a tilted surface	kWh/m <sup>2</sup> /day
$K_T$	Clearness index (ratio of global radiation to extraterrestrial radiation)	–
$R_b$	Ratio of beam radiation on the tilted surface to that on the horizontal surface	–
$R_d$	Ratio of diffuse radiation on the tilted surface to that on the horizontal surface	–
$\rho_g$	Ground reflectance (albedo)	–
$G_T$	Solar irradiance incident on the PV panel surface	W/m <sup>2</sup>
$G_{STC}$	Solar irradiance at Standard Test Conditions	W/m <sup>2</sup>
$T_c$	Photovoltaic cell temperature	°C
$T_a$	Ambient air temperature	°C
$T_{STC}$	Cell temperature at Standard Test Conditions	°C
$T_{c,NOCT}$	Cell temperature at nominal operating cell temperature conditions	°C
$T_{a,NOCT}$	Ambient temperature at NOCT conditions	°C
$G_{T,NOCT}$	Solar irradiance at NOCT conditions	W/m <sup>2</sup>
$P_{pv}$	Estimated photovoltaic system power output	kW
$P_{rated}$	Rated power of the PV system at Standard Test Conditions	kWp
$\gamma$	Temperature coefficient of power	1/°C
$\eta_{mp,STC}$	PV module efficiency at maximum power under STC	–
$\alpha_p$	Temperature coefficient related to PV module performance	1/°C

$\tau$	Transmittance of the PV module cover	–
$\alpha$	Absorptance of the PV cell	–

**Author contributions:** Conceptualization, AAKA, SD and AA; methodology, AA; software, AA; validation, AA; formal analysis, AA; investigation, AA; resources, AA; data curation, AA; writing—original draft preparation, AAKA, SD and AA; writing—review and editing, AAKA, SD and AA; visualization, AA; supervision, AA; project administration, AAKA, SD and AA; funding acquisition, AAKA, SD and AA. All authors have read and agreed to the published version of the manuscript.

**Funding:** This work received no external funding

**Institutional review board statement:** Not applicable.

**Informed consent statement:** Not applicable.

**Data availability statement:** Not applicable.

**Conflict of interest:** The authors declare no conflict of interest.

## References

1. International Renewable Energy Agency (IRENA). Global Renewables Outlook: Energy Transformation 2050. IRENA; 2020. Available online: <https://www.irena.org/publications/2020/Apr/Global-Renewables-Outlook-2020>
2. International Renewable Energy Agency (IRENA). Future of Solar Photovoltaic: Deployment, Investment, Technology, Grid Integration and Socio-Economic Aspects. IRENA; 2019. Available online: <https://www.irena.org/publications/2019/Nov/Future-of-Solar-Photovoltaic>
3. International Renewable Energy Agency (IRENA). Renewable Capacity Statistics 2020. IRENA; 2020. Available online: <https://www.irena.org/Publications/2020/Mar/Renewable-Capacity-Statistics-2020>
4. International Renewable Energy Agency (IRENA). Renewable Power Generation Costs in 2019. IRENA; 2019. Available online: <https://www.irena.org/publications/2020/Jun/Renewable-Power-Costs-in-2019>
5. Mansour RB, Mateen Khan MA, Alsulaiman FA, et al. Optimizing the Solar PV Tilt Angle to Maximize the Power Output: A Case Study for Saudi Arabia. *IEEE Access*. 2021; 9: 15914–15928. doi: 10.1109/ACCESS.2021.3052933
6. Taghavi M, Lee CJ. Development of a novel hydrogen liquefaction structure based on liquefied natural gas regasification operations and solid oxide fuel cell: Exergy and economic analyses. *Fuel*. 2025; 384: 133826. doi: 10.1016/j.fuel.2024.133826
7. Hepbasli A, Alsuhaibani Z. A key review on present status and future directions of solar energy studies and applications in Saudi Arabia. *Renewable and Sustainable Energy Reviews*. 2011; 15(9): 5021–5050. doi: 10.1016/j.rser.2011.07.052
8. Hafez AZ, Soliman A, El-Metwally KA, et al. Tilt and azimuth angles in solar energy applications—A review. *Renewable and Sustainable Energy Reviews*. 2017; 77: 147–168. doi: 10.1016/j.rser.2017.03.131
9. Taghavi M, Yoon HJ, Choi JU, et al. Innovative Structure of a Liquefied Natural Gas (LNG) Process by Mixed Fluid Cascade Using Solar Renewable Energy, Photovoltaic Panels (PV), and Absorption Refrigeration System. In: *Computer Aided Chemical Engineering*. Elsevier; 2024. pp. 2071–2076. doi: 10.1016/B978-0-443-28824-1.50346-X
10. Khatib T, Mohamed A, Mahmoud M, et al. Optimization of the Tilt Angle of Solar Panels for Malaysia. *Energy Sources, Part A: Recovery, Utilization, and Environmental Effects*. 2015; 37(6): 606–613. doi: 10.1080/15567036.2011.588680
11. Hailu G, Fung AS. Optimum Tilt Angle and Orientation of Photovoltaic Thermal System for Application in Greater Toronto Area, Canada. *Sustainability*. 2019; 11(22): 6443. doi: 10.3390/su11226443
12. Taghavi M, Lee CJ. Development of novel hydrogen liquefaction structures based on waste heat recovery in diffusion-absorption refrigeration and power generation units. *Energy Conversion and Management*. 2024; 302: 118056. doi: 10.1016/j.enconman.2023.118056

13. Shukla KN, Rangnekar S, Sudhakar K. Comparative study of isotropic and anisotropic sky models to estimate solar radiation incident on tilted surface: A case study for Bhopal, India. *Energy Reports*. 2015; 1: 96–103. doi: 10.1016/j.egy.2015.03.003
14. Glick A, Ali N, Bossuyt J, et al. Utility-scale solar PV performance enhancements through system-level modifications. *Scientific Reports*. 2020; 10(1): 10505. doi: 10.1038/s41598-020-66347-5
15. Abdeen E, Orabi M, Hasaneen ES. Optimum tilt angle for photovoltaic system in desert environment. *Solar Energy*. 2017; 155: 267–280. doi: 10.1016/j.solener.2017.06.031
16. Jacobson MZ, Jadhav V. World estimates of PV optimal tilt angles and ratios of sunlight incident upon tilted and tracked PV panels relative to horizontal panels. *Solar Energy*. 2018; 169: 55–66. doi: 10.1016/j.solener.2018.04.030
17. Abdallah R, Juaidi A, Abdel-Fattah S, et al. Estimating the Optimum Tilt Angles for South-Facing Surfaces in Palestine. *Energies*. 2020; 13(3): 623. doi: 10.3390/en13030623
18. Yunus Khan TM, Soudagar M, Kanchan M, et al. Optimum location and influence of tilt angle on performance of solar PV panels. *Journal of Thermal Analysis and Calorimetry*. 2020; 141(1): 511–532. doi: 10.1007/s10973-019-09089-5
19. Murtaza AF, Munir U, Chiaberge M, et al. Variable Parameters for a Single Exponential Model of Photovoltaic Modules in Crystalline-Silicon. *Energies*. 2018; 11(8): 2138. doi: 10.3390/en11082138
20. Klein SA, Theilacker JC. An Algorithm for Calculating Monthly-Average Radiation on Inclined Surfaces. *Journal of Solar Energy Engineering*. 1981; 103(1): 29–33. doi: 10.1115/1.3266201
21. Adam A, Kaçar F. Simulation of Induction Motor Driving by Bridge Inverter at 120°, 150°, and 180° Operation. In: *Proceedings of the 2021 8th International Conference on Electrical and Electronics Engineering (ICEEE)*; 9 April 2021; Antalya, Turkey. pp. 121–125. doi: 10.1109/ICEEE52452.2021.9415930
22. Yadav AK, Chandel SS. Tilt angle optimization to maximize incident solar radiation: A review. *Renewable and Sustainable Energy Reviews*. 2013; 23: 503–513. doi: 10.1016/j.rser.2013.02.027
23. Alahmad A, Kaçar F, Uzunoğlu CP. Medium Voltage Drives (MVD)–Design and Configuration of Eighteen-Pulse Phase Shifting Autotransformer Rectifier for Cascaded H-Bridge Motor Driver Application. *Electric Power Components and Systems*. 2024; 1–8. doi: 10.1080/15325008.2023.2296962
24. Alahmad A, Kaçar F, Uzunoğlu CP. Comprehensive Analysis of DC Link Capacitors Used in Cascaded H-Bridge Motor Driver. *Electric Power Components and Systems*. 2024; 1–11. doi: 10.1080/15325008.2024.2357262
25. Adam A, Kacar F, Mastorakis N. Enhancement design of eleven-level cascaded h-bridge motor driver application. *Computers and Electrical Engineering*. 2025; 123: 110179. doi: 10.1016/j.compeleceng.2025.110179
26. Diab S, Adam A. Design and modelling of solar water pumping system for irrigation in Syria, Damascus. *Energy Storage and Conversion*. 2025; 3(3). doi: 10.59400/esc3849
27. Al-Bashir A, Al-Dweri M, Al-Ghandoor A, et al. Analysis of effects of solar irradiance, cell temperature and wind speed on photovoltaic systems performance. *International Journal of Energy Economics and Policy*. 2020; 10(1): 353–359. doi: 10.32479/ijee.8591
28. Samer D, Adil A. Enhanced solar energy conversion for direct current motor speed control. *i-manager's Journal on Electrical Engineering*. 2025; 19(1): 1. doi: 10.26634/jee.19.1.22258
29. Al Garni HZ, Awasthi A, Wright D. Optimal orientation angles for maximizing energy yield for solar PV in Saudi Arabia. *Renewable Energy*. 2019; 133: 538–550. doi: 10.1016/j.renene.2018.10.048
30. Fytianos G, Vevelstad SJ, Knuutila HK. Degradation and corrosion inhibitors for MEA-based CO<sub>2</sub> capture plants. *International Journal of Greenhouse Gas Control*. 2016; 50: 240–247. doi: 10.1016/j.ijggc.2016.05.003
31. Manaf ND, Fukuda K, Subhi ZA, et al. Influences of surface roughness on the water adsorption on austenitic stainless steel. *Tribology International*. 2019; 136: 75–81. doi: 10.1016/j.triboint.2019.03.014
32. Zhao F, Cui C, Dong S, et al. An overview on the corrosion mechanisms and inhibition techniques for amine-based post-combustion carbon capture process. *Separation and Purification Technology*. 2023; 304: 122091. doi: 10.1016/j.seppur.2022.122091
33. Lepaumier H, Da Silva EF, Einbu A, et al. Comparison of MEA degradation in pilot-scale with lab-scale experiments. *Energy Procedia*. 2011; 4: 1652–1659. doi: 10.1016/j.egypro.2011.02.037
34. Da Silva EF, Lepaumier H, Grimstvedt A, et al. Understanding 2-Ethanolamine Degradation in Postcombustion CO<sub>2</sub> Capture. *Industrial & Engineering Chemistry Research*. 2012; 51(41): 13329–13338. doi: 10.1021/ie300718a
35. Knudsen JN, Andersen J, Jensen JN, et al. Evaluation of process upgrades and novel solvents for the post combustion CO<sub>2</sub> capture process in pilot-scale. *Energy Procedia*. 2011; 4: 1558–1565. doi: 10.1016/j.egypro.2011.02.025
36. Jørsboe JK, Vinjarapu SHB, Neerup R, et al. Mobile pilot plant for CO<sub>2</sub> capture in biogas upgrading using 30 wt% MEA. *Fuel*. 2023; 350: 128702. doi: 10.1016/j.fuel.2023.128702

37. Meenakshi T, Vanitha NS. Modified multilevel Quasi Z inverter for solar irrigation systems with improved control technique. In: *Proceedings of the 2017 International Conference on Advances in Electrical Technology for Green Energy (ICAETGT)*; 23 September 2017; Coimbatore, India. pp. 139–148. doi: 10.1109/ICAETGT.2017.8341467
38. Stonier AA, Murugesan S, Samikannu R, et al. Power Quality Improvement in Solar Fed Cascaded Multilevel Inverter With Output Voltage Regulation Techniques. *IEEE Access*. 2020; 8: 178360–178371. doi: 10.1109/ACCESS.2020.3027784
39. Kala P, Arora S. Implementation of Hybrid GSA SHE Technique in Hybrid Nine-Level Inverter Topology. *IEEE Journal of Emerging and Selected Topics in Power Electronics*. 2021; 9(1): 1064–1074. doi: 10.1109/JESTPE.2019.2963239
40. Fahad M, Tariq M, Sarwar A, et al. Asymmetric Multilevel Inverter Topology and Its Fault Management Strategy for High-Reliability Applications. *Energies*. 2021; 14(14): 4302. doi: 10.3390/en14144302
41. Dhanamjayulu C, Khasim SR, Padmanaban S, et al. Design and Implementation of Multilevel Inverters for Fuel Cell Energy Conversion System. *IEEE Access*. 2020; 8: 183690–183707. doi: 10.1109/ACCESS.2020.3029153